Korea-Australia Rheology Journal
Vol. 20, No. 4, December 2008 pp. 235-243

Development of polypropylene-clay nanocomposite with supercritical CO_2 assisted twin screw extrusion

Tae Yong Hwang[1], Sang Myung Lee[2], Youngjoon Ahn[1] and Jae Wook Lee[1,*]
[1]*Department of Chemical and Biomolecular Engineering, Sogang University, Seoul, 121-742, Korea*
[2]*LG Micron Ltd., Gupo-dong, Gumi-city, Gyeongsang buk-do, 730-713, Korea*
(Received October 8, 2008; final revision received November 21, 2008)

Abstract

The aim of this study is to explore the possibility of incorporating supercritical carbon dioxide ($scCO_2$) into twin screw extrusion process for the production of polypropylene-clay nanocomposite (PPCN). The CO_2 is used as a reversible plasticizer which is expected to rapidly transport polymeric chains into the galleries of clay layers in its supercritical condition inside the extruder barrel and to expand the gallery spacings in its sub-critical state upon emerging from die. The structure and properties of the resulting PPCNs are characterized using wide-angle X-ray diffraction (WAXD), transmission electron microscopy (TEM), rheometry, thermogravimetry and mechanical testing. In the processing of the PPCNs with $scCO_2$, optimum $scCO_2$ concentration and screw speed which maximized the degree of intercalation of clay layers were observed. The WAXD result reveals that the PP/PP-g-MA/clay system treated with $scCO_2$ has more exfoliated structure than that without $scCO_2$ treatment, which is supported by TEM result. $ScCO_2$ processing enhanced the thermal stability of PPCN hybrids. From the measurement of linear viscoelastic property, a solid-like behavior at low frequency was observed for the PPCNs with high concentration of PP-g-MA. The use of $scCO_2$ generally increased Young's modulus and tensile strength of PPCN hybrids.

Keywords : polypropylene clay nanocomposite, supercritical fluid, twin screw extrusion

1. Introduction

Composite materials that contain a nanometer scale filler have been appeared over the last 15 years to afford remarkable property enhancements relative to conventionally-scaled composites (Schmidt, 1985; Novak, 1993; Mark, 1996). A polymer layered silicate nanocomposite where layered silicates of nano-scale dimensions are dispersed as a reinforcing phase in an engineering polymer matrix is one of the most important forms of "hybrid organic-inorganic nanocomposites" (Okada and Usuki, 1995; Giannelis, 1996; Ogawa and Kuroda, 1997). The composite with well dispersed silicate layers exhibit a significant improvement in thermal, mechanical, barrier properties with the use of minimal amount of filler. Many polymeric systems have been investigated in this field, such as polyamide 6 (Giannelis, 1996; Kojima *et al.*, 1993), polystyrene (Zax *et al.*, 2000; Vaia *et al.*, 1993), polyethylene terephthalate (Ke *et al.*, 1999; Davis *et al.*, 2002), polycaprolactone (Messersmith and Giannelis, 1995; Jimenez *et al.*, 1997), and epoxy resin (Messersmith and Giannelis, 1994; Lan *et al.*, 1995), *etc.* It was found that the exfoliated/intercalated dispersion of the clay layers could be achieved in certain polymers, which have polar functional groups compatible with the polar hydroxyl groups on the silicate clay layers.

Polypropylene is one of the most widely used thermoplastic materials in the plastics industry. A successfully developed PP/clay nanocomposite has a great potential being applied in the diverse areas of industry such as automobile, bottle, film, and package, *etc.* However, because of the non-polar nature of the polypropylene, it is difficult to exfoliate silicate layers and to have homogeneous dispersion of the silicate layers in PP matrix. This is because the organophilic clays have polar hydroxyl groups and are compatible only with polymers containing polar functional groups. To resolve the incompatibility between nonpolar polymer and polar clay, compatibilizers such as PP-g-MA and hydroxyl groups grafted polypropylene were used. These compatibilizers contain polar functional groups which enhance the interface interaction between the PP matrix and the clay layers (Usuki *et al.*, 1997; Fischer and Gielgens, 1999).

Supercritical fluids have the characteristics of gas-like diffusivity, liquid-like density, low viscosity and surface tension. Supercritical fluids have received a great deal of attention as an efficient processing aid for the synthesis and processing polymeric materials Tae Yong Hwang, Sang

*Corresponding author: jwlee@sogang.ac.kr

Myung Lee, Youngjoon Ahn and Jae Wook Lee. The supercritical fluids can plasticize most of polymers efficiently and can be easily removed after depressurization acting as a "reversible plasticizer" (Brennecke, 1997). Among the supercritical fluids, $scCO_2$ has been used in a wide range of applications due to its environmentally friendliness, low critical point (31.1°C, 73.8 bar), relatively low cost, non-toxic nature, and non-flammability.

There have been various attempts to incorporate $scCO_2$ into continuous processing system to enhance the dispersion of clay layers of nanocomposite. Manke *et al.* (2002) patented a method to delaminate a layered silicate material by supercritical fluid treatment. The method includes contacting the layered silicate with the supercritical fluid and catastrophically depressurizing the contacted layered silicate particle to exfoliate the layered particles. The supercritical treated particles were mixed with a polymer to form a reinforced nanocomposite. Mielewski *et al.* (2002) patented a method of preparing a reinforced polymer by supercritical fluid treatment. In the method the layered silicate was mixed with a polymer to form a treatable silicate-polymer mixture and the mixture was contacted with supercritical fluid to exfoliate the silicate particles so that the particles disperse within the polymer. Garcia-Leiner (2004) recently reported data for a polyethylene-MMT nanocomposite processed in a modified single screw extruder equipped with $scCO_2$ injection near the feed hopper. Their results show a 40~100% increase in basal spacing and suggest that $scCO_2$ processing plays a significant role in facilitating melt intercalation and clay dispersion. Treece and Oberhauser (2007) investigated two different melt-blending strategies which are conventional TSE and single-screw extrusion capable of direct $scCO_2$ feed to extruder barrel. They concluded that the high shear of the twin screw process is vastly superior to the single-screw with in-line $scCO_2$ addition in generating well-exfoliated, percolated PP-clay nanocomposites.

The twin screw extruder is generally less advantageous in building up the high pressure required to provide the supercritical condition compared to single screw extruder. However, through a judicious design of screw configuration, a significant build up of pressure can be achieved before and after the supercritical fluid injection point and the melt seal to prevent leakage of $scCO_2$ can be formed. Referring to numerous solubility studies, it is expected that only a limited amount of CO_2 is required to plasticize polymeric melt and to enhance the diffusion of polymer chains. Furthermore twin screw extruder is an excellent mixer which is well suited to dissolve $scCO_2$ into the PP melt in relatively short distance of the barrel.

In this study we introduced $scCO_2$ directly into the midstream of twin screw extruder to produce the PP/clay nanocomposite with enhanced dispersion of clay layers. The $scCO_2$ was used as a reversible plasticizer which is

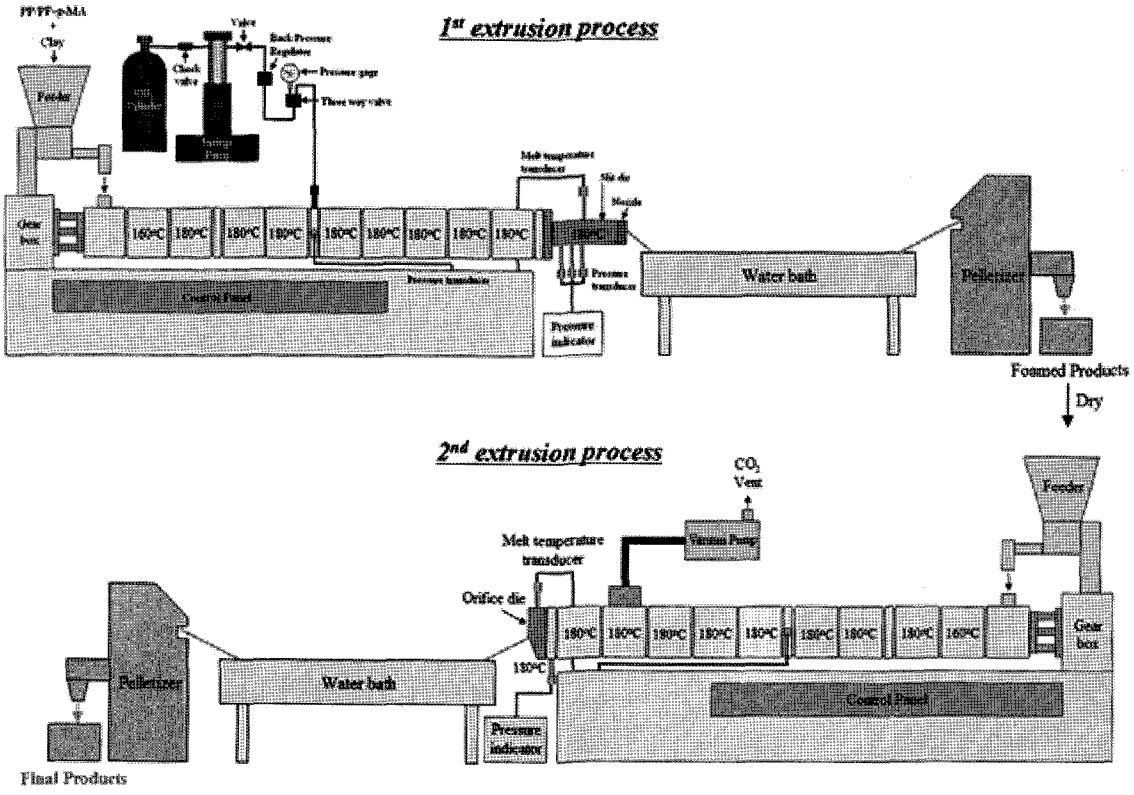

Fig. 1. Schematic of $scCO_2$ assisted twin screw extrusion process.

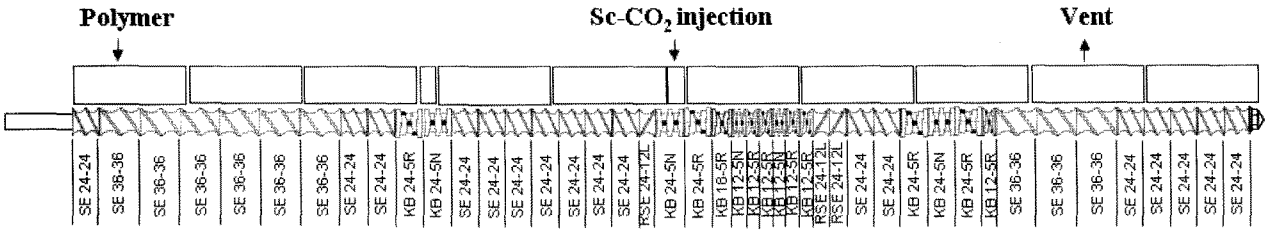

Fig. 2. Screw and barrel configurations.

expected to enhance the diffusion of polymer chains into the galleries of silicate layers in the extruder barrel and expand the gallery spacing by significant depressurization at the exit of die. The effects of concentrations of $scCO_2$, clay, and PP-g-MA and screw speed on the properties of the nanocomposite are studied. A comparison between conventional nanocomposite and the nanocomposite processed with $scCO_2$ was made.

2. Experimental

2.1. Materials

The matrix polymer used was polypropylene (HP602N, Polymirae) with density of 0.9 g/cm^3, MFR of 12.5 g/10 min, $\overline{M}_w$=222,400 and $\overline{M}_w/\overline{M}_n$=5.23. Maleic anhydride modified polypropylene (Fusabond MD 353D, Dupont) with MA content of 3.2 wt% was used as a compatibilizer. A processing antioxidant (Irganox 8225, Ciba Specialty Chemicals) was used. The organically modified montmorillonite (Cloisite 20A, Southern Clay Products) was used as a nanoscale filler. The Cloisite 20A(C20A) was a montmorillonite ion-exchanged with dimethyl dehydrogenated tallow ammonium ions, where tallow was composed predominantly of octadecyl chains with smaller amount of lower homologues. The approximate composition was C18 (65%), C16 (30%), and C14 (5%). All materials were dried under vacuum at 80°C prior to the processing.

2.2. Procedure

Table 1. Compositions of polypropylene nanocomposite

Sample	PP (part)	PP-g-MA (part)	C20A (part)
PPCN1	100	0	3
PPCN2	100	0	5
PPCN3	98	2	5
PPCN4	95	5	5
PPCN5	90	10	5
PPCN6	85	15	5
PPCN7	75	25	5

The melt extrusion was performed in a co-rotating, intermeshing twin screw extruder (SM TEK25, SM Platek Korea) with a diameter of 25 mm and a ratio of screw length to diameter (L/D) of 41. The extruder setup and screw configuration are shown in Figs. 1 and 2. For precise $scCO_2$ feeding into the extruder barrel, a metered $scCO_2$ injection system shown in Fig. 1 was devised. It is composed of a CO_2 cylinder, a syringe pump (Model 260D, ISCO, Inc.) and a back pressure regulator. The Syringe pump was set to have a constant flow rate and the back pressure regulator was used for the stable supply of $scCO_2$ into the extruder barrel. The processing of PP/clay nanocomposite was performed by two step extrusion process. (see Fig. 1) In the first step, PP and clay were blended in the extruder with $scCO_2$ injected into the middle of the extruder barrel and the foamed PP/clay mixture was obtained. In order to build up the pressure above the critical pressure (73.8 bar) of CO_2, a nozzle was used in a slit die. The resulting highly foamed extrudate was cooled and pelletized. In the second step, the foamed PP/clay was re-extruded with venting enabled to remove bubbles and to further disperse clay layers in the matrix. The operating temperature profile for the extruder varied from 140°C at the feed section to 180°C at the die. The screw was arranged in a special combination of conveying, shearing, mixing, and reversing elements as shown in Fig. 2. Reverse screw elements were inserted before and after the $scCO_2$ injection point to provide melt sealing. The PP/clay nanocomposite without $scCO_2$ was extruded at the same processing condition. The compositions of PP/clay hybrids tested are shown in Table 1. For brevity, the composition of the PPCN hybrid will be designated as (part PP/part PP-g-MA/part C20A).

2.3. Characterization of PP/clay nanocomposite

Structural characterization was carried out utilizing X-ray diffraction (XRD) and transmission electron microscope (TEM).

X-ray diffraction experiments were performed using Rigaku D/Max-A diffractometer (Cu Kα radiation with λ= 1.5406 Å) at room temperature. The 2θ angles were varying between 1.5 and 10° at a scanning rate of 1°/min in order to measure the d_{001}-spacing between silicate layers. The generator was operated at 40 kV and 40 mA. Test specimens

were prepared by compression molding at 180°C.

Transmission electron microscope (TEM), Carl Zeiss LEO 912AB, was used to observe the dispersion of silicate in nanocomposites at an acceleration voltage of 160kV. Nanometer sections are prepared from the pellets via melt compounded on the twin-screw extruder. Ultrathin sections of 100 nm in thickness, mounted on a 200 mesh copper grid, are cut using a microtome (Leica EM FCS) procedure with a diamond knife where the sample is held at room temperature to produce the uniform thin sections required to obtain clear reproducible images.

The thermal gravimetric analyzer (TGA, TGA2950 from TA Inc.) was used to evaluate the thermal stability of the PP/clay nanocomposites. The chamber was purged with nitrogen. The temperature range was between 40 and 700°C, and the heating rate was 20°C/min.

Tensile test of nanocomposite was carried out using a universal testing machine (UTM, LR-5K from Lloyd Co.) with 500 kg_f load cell. The crosshead speed was fixed at 50 mm/min for all of the specimens and measurements for each case were performed more than at least 5 times. The dimension of the test sample corresponds to ASTM D638 (type V).

3. Results and discussion

3.1. Effect of $scCO_2$ on silicate layer dispersion

Fig. 3 shows the XRD patterns for organoclay C20A and PPCN1 (100/0/3) hybrids extruded with various loadings of $scCO_2$. The (001) plane peak of PPCN1 extruded without $scCO_2$ was observed at $2\theta=3.40°$ which corresponds to the basal spacing of 26.0 Å, calculated from Bragg's law, while the peak of the organoclay C20A was observed at $2\theta=3.71°$ corresponding to basal spacing of 23.8 Å. The insignificant increment of the basal spacing for PPCN1 without $scCO_2$ can be attributed to the incompatibility of the polar hydroxyl groups on the surface of the silicate layers and the non-polar main chain of PP. The (001) plane peak of PPCN1 extruded with 2 wt% $scCO_2$ has the lowest angle ($2\theta=2.69°$) and thus the largest basal spacing of 32.8 Å which is nearly 26% increase from that of the onga-

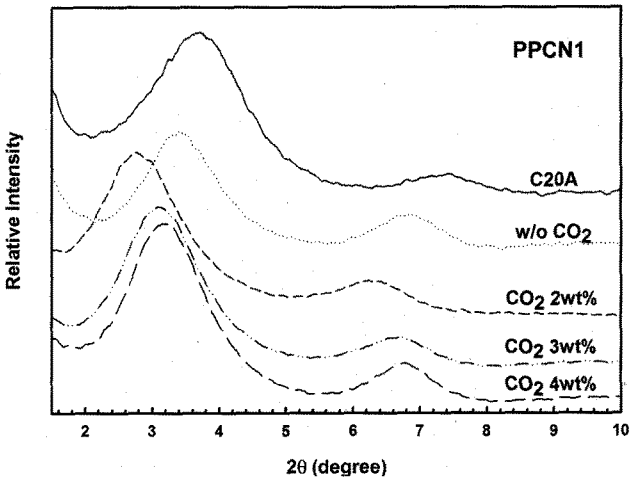

Fig. 3. XRD patterns of PPCN1 as a function of $scCO_2$ concentration (Screw speed 55 rpm).

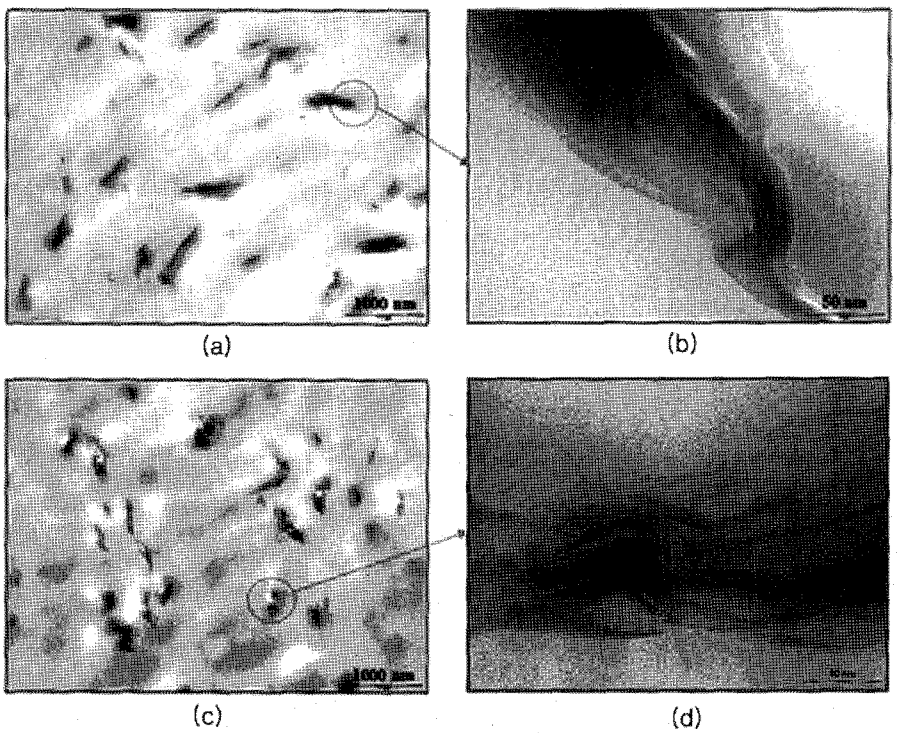

Fig. 4. TEM image of PPCN1. (a), (b) processed without CO_2, (c), (d) processed with 2 wt% CO_2.

noclay in the nanocomposite extruded without $scCO_2$. But further increase of $scCO_2$ content decreased the basal spacing. The XRD result can be complemented or confirmed by TEM analysis. Fig. 4 shows TEM images of PPCN1s processed without $scCO_2$ and with 2 wt% $scCO_2$. From low magnification TEM images, Figs. 4(a) and 4(c), it is seen that compared with those of PPCN1 samples processed without $scCO_2$, tactoids of PPCN1 samples processed with $scCO_2$ become smaller in size and larger in number. To observe detailed clay layer arrangement within a tactoid, high magnification TEM images are presented in Figs. 4(b) and 4(d). For PPCN1 processed without $scCO_2$, individual tactoid is composed of tightly bound silicate layers. For PPCN1 processed with 2% $scCO_2$, layer spacings are enlarged and some exfoliated silicate layers can be seen. This TEM result indicates that $scCO_2$ can be an effective dispersant for the dispersion of clay layers in PP matrix. It seems that $scCO_2$ enhances the diffusion rate of PP-$ScCO_2$ mixture into the galleries of silicate layers and lower the surface tension between the polymer and the clay. Furthermore, the mixture of PP-clay-$scCO_2$ will experience significant pressure depression and volume expansion as it passes through a die, and this may help the clay layers fall apart. A similar result as shown in Fig. 4 was obtained for the PPCN2 (100/0/5) hybrid. The increase of $scCO_2$ concentration in PP melt results in the enhanced diffusion and thus intercalation of PP molecules into the galleries of clay layers but also makes it difficult to maintain melt seal within the $scCO_2$ dissolution screw zone due to the $scCO_2$ plasticated low pressure melt. The lowered viscosity of the $scCO_2$ dissolved PP melt is certainly not a favorable condition to break larger tactoids to smaller ones and exfoliate tactoids to individual clay layers. It seems that because of the two competing effects, there exists an optimum $scCO_2$ concentration of 2 wt% where the intercalation of clay is maximized.

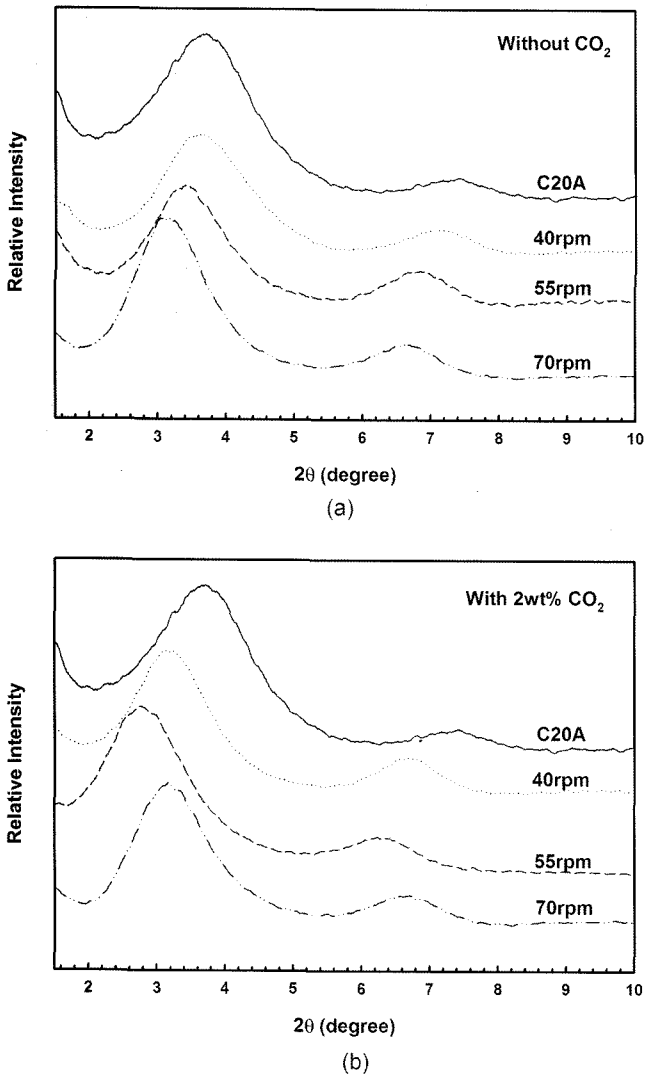

Fig. 5. XRD pattern of PPCN1 as a function of screw speed. (a) processed without CO_2, (b) processed with 2 wt% CO_2.

3.2. Effects of screw speed on silicate layer dispersion

Figs. 5(a) and 5(b) show XRD patterns of PPCN1 extruded without $scCO_2$ and with 2 wt% $scCO_2$, respectively, as a function of screw speed. In case of PPCN1 without CO_2, as screw speed is increased, gallery distance was increased due to the increased stress level which promotes the dispersion of clay layers. But interestingly, in case of PPCN1 with 2 wt% CO_2, the degree of intercalation for PPCN1 was maximized at screw speed of 55 rpm. The decreasing degree of intercalation for PPCN1 at screw speed of 70 rpm can be attributed to the reduction of the residence time, which is not enough for the PP chains to diffuse into galleries of silicate layers.

3.3. Effects of PP-g-MA on clay exfoliation

Using $scCO_2$ it was possible to produce PP/organoclay nanocomposite with intercalated structure. To overcome the incompatibility of the polar hydroxyl groups on the surface of the clay layers and the non-polar PP and thus to achieve an improved dispersion state in the PPCNs, PP-g-MA is commonly used as a compatibilizer. Therefore, to further enhance the dispersion state of PP/clay hybrids and to have possible synergetic effect, $scCO_2$ and PP-g-MA was used together. Fig. 6(a) shows XRD patterns of PPCNs extruded without $scCO_2$ for various PP-g-MA concentrations. The (001) plane peak of clay is reduced and is shifted to the lower angle as PP-g-MA concentration is increased. PPCN2 having no PP-g-MA exhibits small peak angle shift and no significant intensity change indicating that limited intercalation of silicate layers has occurred in PPCN2. From PPCN3 (98/2/5) to PPCN5 (90/10/5) as PP-g-MA concentration increases the peak shifts to lower angle and the peak intensity is decreased which means the gallery spacing is increased and more disordered/exfoliated structure is created. In XRD curves of PPCN6 (85/15/5)

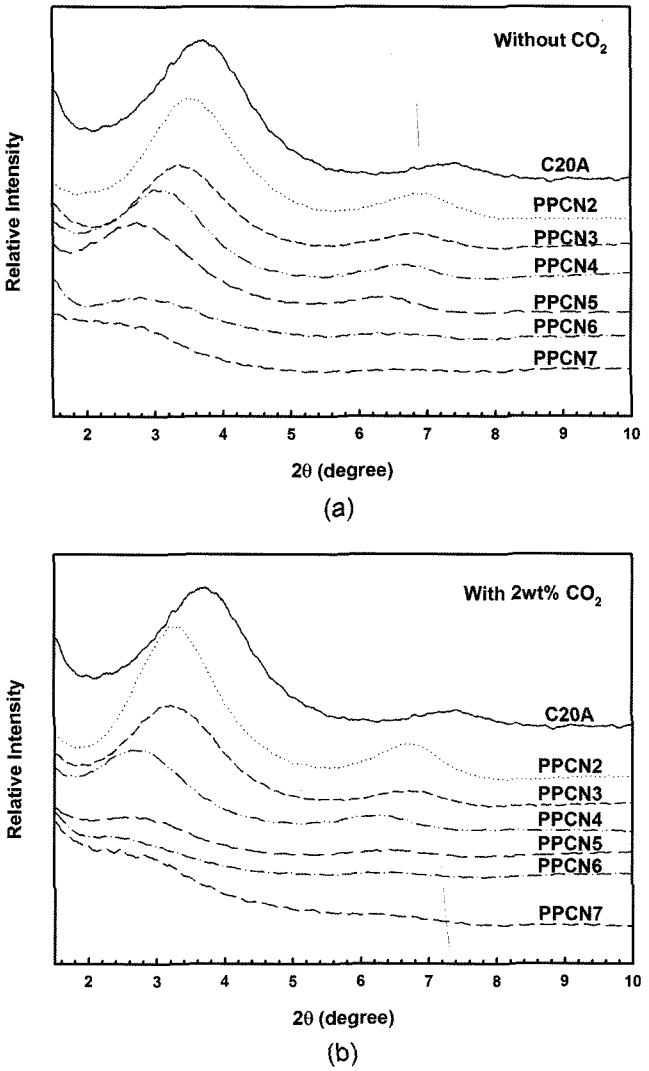

Fig. 6. XRD pattern of PPCN as a function of PP-g-MA concentration. (a) processed without CO_2, (b) processed with 2 wt% CO_2.

and PPCN7 (75/25/5) the peak was almost disappeared and this can be attributed to the highly disordered or exfoliated structure of silicate layers in the hybrids. Fig. 6(b) shows XRD patterns of PPCNs extruded with 2 wt% CO_2 as a function of PP-g-MA concentration. The peak was almost disappeared for PPCN5, PPCN6 and PPCN7. Note that whereas PPCN5 hybrid with no $scCO_2$ treatment was intercalated, the same hybrid with $scCO_2$ treatment was almost exfoliated.

Figs. 7(a)-(f) show TEM photomicrographs of PPCNs extruded with and without $scCO_2$. Note the different magnifications for PPCN hybrids; 12000 for (a), 24000 for (b) through (e), and 37500 for (f). In Fig. 7(a) even larger clusters of clay are observed in PPCN2 with $scCO_2$ and without $scCO_2$ indicating poor dispersion of clay layers in PP matrix without PP-g-MA. From Figs. 7(b) and 7(c), the size of the clusters for PPCN3 and 4 became considerably

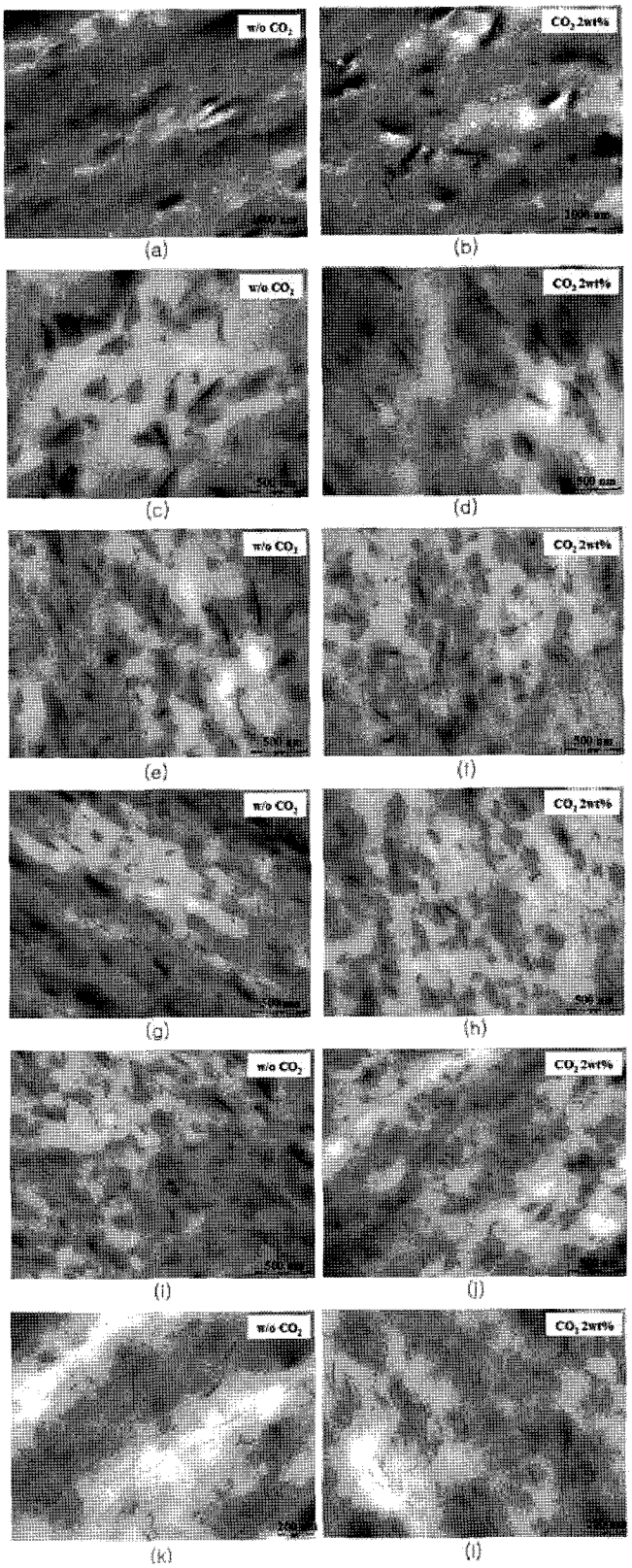

Fig. 7. TEM images of PPCNs as a function of PP-g-MA concentration. (a),(b): PPCN2, (c),(d): PPCN3, (e),(f): PPCN4, (g),(h): PPCN5, (i),(j): PPCN6, (k),(l): PPCN7; left side: processed without CO_2; right side: processed with 2 wt% CO_2.

smaller compared with that for PPCN2. But the difference between $scCO_2$ treated and untreated is not clear. In Figs. 7(d)-7(f), we can observe the improved dispersion of the PPCN hybrids processed with $scCO_2$ compared with those without $scCO_2$. A few of clusters or tactoids can be encountered but majority of the clay exists as exfoliated layers. Generally, as the PP-g-MA concentration increases it is observed that the dispersion state of silicate layers is improved especially at high concentration of PP-g-MA. Also, while the big clusters of clay appear in the PPCNs extruded without $scCO_2$ the clusters are broken to smaller ones in the PPCNs extruded with $scCO_2$. This indicates that $scCO_2$ is effective when it is applied with high concentration of PP-g-MA.

3.4. Linear viscoelastic properties

From the storage modulus vs. frequency plots for pure PP and PPCN hybrids processed without and with $scCO_2$ significant enhancement of the storage moduli of the

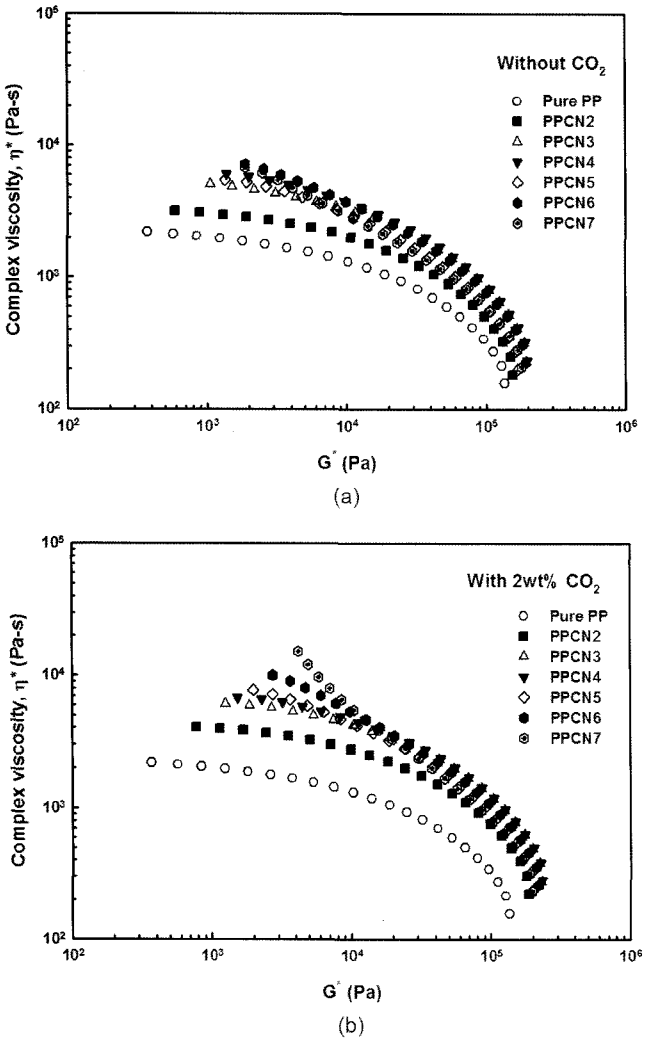

Fig. 8. Cross plot for pure PP and PPCN hybrids. (a) processed without $scCO_2$, (b) processed with $scCO_2$.

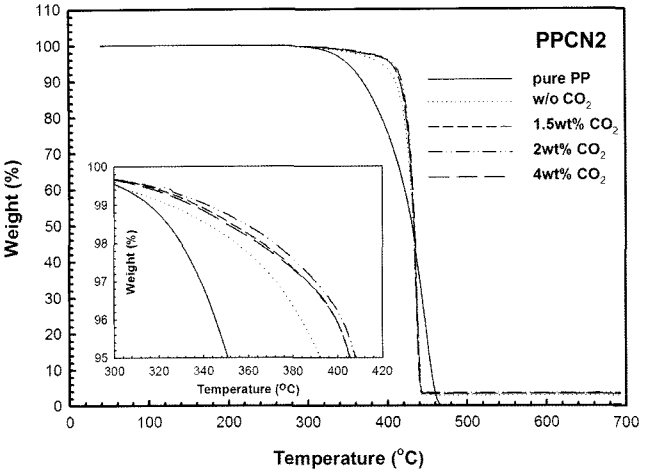

Fig. 9. TGA curves of PPCN2 hybrids as a function of CO_2 concentration.

PPCN hybrids at low frequency as the PP-g-MA concentration was increased and the non-terminal behavior which is typically attributed to the three dimensional percolated network structure (Galgali *et al.*, 2001; Solomon *et al.*, 2001) at the high concentration of PP-g-MA were observed (data not shown for brevity). A cross-plot is constructed from the result of the small amplitude oscillatory measurement and is shown in Fig. 8 for PPCNs without CO_2 and PPCNs with CO_2. The cross-plot for PPCN7 processed with $scCO_2$ shows the divergence of η^* at finite values of G^* which is indicative of the solid-like nature exhibited by some exfoliated nanocomposites with good polymer-clay interactions (Xu *et al.*, 2005).

3.5. Thermal stability of PPCNs

The thermal stability of nanocomposites is studied by thermogravimetric analysis (TGA). When the heating occurs under an inert gas flow, a non-oxidative degradation occurs, while the use of air or oxygen allows oxidative degradation of the samples. In general thermal stability of nanocomposites is enhanced by physical protective barrier created by the reassembling of silicate layers on the surface of nanocomposites and delayed volatilization due to the labyrinth effect of silicate layers dispersed in the matrix polymer (Gilnian *et al.*, 1998). Fig. 9 represents the result of TGA analysis for PPCN2 as a function of $scCO_2$ concentration compared with neat PP. It is seen that PPCN2 hybrids processed with $scCO_2$ have superior thermal stability compared with neat PP and PPCN2 with 2 wt% $scCO_2$ has the highest thermal stability. As mentioned previously in XRD result, PPCN2 had a maximum interlayer distance when $scCO_2$ concentration was 2 wt%. Although the most desirable structure of the nanocomposites for a good thermal stability may be the exfoliated structure, intercalated structure may contribute to the enhancement in thermal stability of the nanocomposite. Thus this TGA

result is well correlated with XRD result in which the layer spacing was maximized at 2 wt% $scCO_2$ concentration. Figs. 10(a) and 10(b) show the TGA results for neat PP and for PPCNs as a function of PP-g-MA concentration processed without CO_2 and with 2 wt% CO_2. Clearly the thermal stability improvement can be seen for the $scCO_2$ treated hybrids. As seen in Fig. 10(a), PPCN composites processed without $scCO_2$ shows progressive increase in thermal stability. But most of the PPCN hybrids (from PPCN3 through PPCN6) processed with $scCO_2$ have the almost the same thermal stability. Note that PPCN7 composite has the highest thermal stability which is well correlated with the previous rheometry result. The fact that the PPCN composites processed with $scCO_2$ have improved thermal stabilities compared with the counterparts without $scCO_2$ can be attributed to the disordered and/or exfoliated structure of the PPCN composites processed with $scCO_2$.

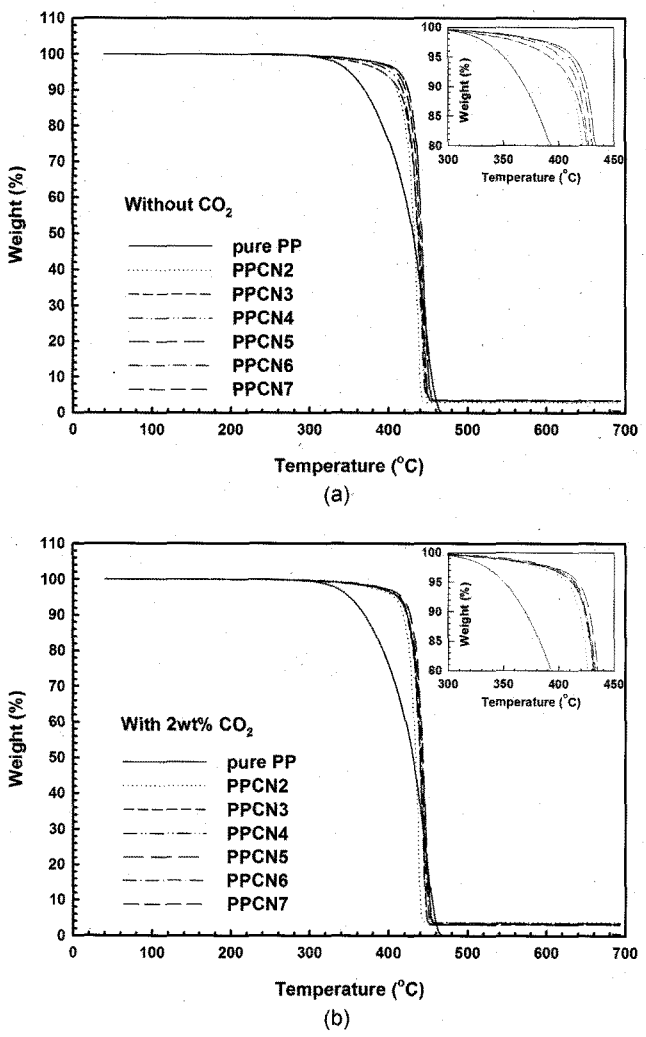

Fig. 10. Thermal stabilities of PPCNs as a function of PP-g-MA concentration. (a) without CO_2, (b) with 2 wt% CO_2.

Table 2. Mechanical properties of PPCNs measured by UTM

Sample	Young's modulus (Mpa)	Stiffness (N/m)	Tensile strength (Mpa)
PPCN2 (Without CO_2)	369 (1.26)	127511 (0.93)	28.8 (0.91)
PPCN3	394 (1.35)	130742 (0.96)	31.5 (1)
PPCN4	380 (1.30)	173410 (1.27)	31.4 (0.99)
PPCN5	406 (1.39)	138333 (1.01)	29.5 (0.94)
PPCN6	418 (1.43)	137906 (1.01)	32.4 (1.03)
PPCN7	430 (1.47)	145636 (1.07)	30.4 (0.97)
PPCN2 (2 wt% CO_2)	423 (1.44)	180829 (1.32)	33.1 (1.05)
PPCN3	455 (1.55)	167863 (1.23)	37.5 (1.19)
PPCN4	436 (1.49)	140894 (1.03)	30.1 (0.96)
PPCN5	435 (1.49)	158293 (1.16)	28.1 (0.89)
PPCN6	421 (1.44)	142649 (1.04)	32.0 (1.02)
PPCN7	446 (1.52)	165643 (1.21)	36.3 (1.15)
pure PP	293 (1)	136785 (1)	31.5 (1)

3.6. Mechanical properties of PPCNs

Mechanical properties of PPCNs were evaluated by universal testing machine. Table 2 shows the results of the tensile test of PPCNs processed without and with $scCO_2$. The effect of $scCO_2$ is not profound but it is observed that Young's modulus and tensile strength for the PPCN hybrids processed with $scCO_2$. The main reason for the improvement in Young's modulus and tensile strength in PPCNs processed with $scCO_2$ is due to the high aspect ratio of the clay dispersed in polymer matrix and the strong interaction between matrix and silicate layers via formation of hydrogen bonds.

4. Conclusions

The feasibility of producing PPCN hybrid with enhanced dispersion was explored by employing a method which injected $scCO_2$ directly into the midstream of twin screw extruder. In the processing of the PPCNs with $scCO_2$, optimum $scCO_2$ concentration and screw speed which maximized the degree of intercalation of clay layers were observed. From WAXD result of the PPCN hybrids, an optimum $scCO_2$ concentration at 2 wt% and an optimum screw speed of 55 rpm which give maximum interlayer distance of organoclay in PP matrix were observed. We

could find some positive results for the production of PPCNs with enhanced dispersion property using $scCO_2$. A significant intercalation was achieved for PPCN1 (100/0/3) with 2 wt% $scCO_2$, which was also confirmed by TEM result. The XRD result shows that when $scCO_2$ is used in the PP/PP-g-MA/clay system, more exfoliated structure was observed at high PP-g-MA concentration compared with PP/PP-g-MA/clay system without $scCO_2$ processing. This is supported by TEM result. The thermal stability of PPCN hybrid was improved when it is processed with $scCO_2$. From the measurement of linear viscoelastic property, the PPCN with high concentration of PP-g-MA shows the solid-like nature exhibited by some exfoliated nanocomposites with good polymer-clay interactions. In summary, for the PP/organoclay hybrid the use of $scCO_2$ mainly increased the interlayer distance of the hybrid but for the PP/PP-g-MA/organoclay hybrids the use of $scCO_2$ improved the dispersion state and even enhanced the exfoliation of the hybrid in some cases.

Acknowledgements

Authors are gratefully acknowledging the support by Defense Acquisition Program Administration and Agency for Defence Development. The authors also gratefully acknowledge the Korea Research Foundation Grant for the financial support (KRF-2006-005-J02302).

References

Brennecke, J. F., 1997, Solvents: molecular trees for green chemistry, *Nature* **389**, 333-334.

Davis, C. H., L. J. Mathias, J. W. Gilman, D. A. Schiraldi, J. R. Shields, P. Trulove, T. E. Sutto and H. C. Delong, 2002, Effects of melt-processing conditions on the quality of poly(ethylene terephthalate) montmorillonite clay nanocomposites, *J. Polym. Sci., Part B: Polym. Phys.* **40**, 2661-2666.

Fischer, H. R. and L. H. Gielgens, 1999, Nanocomposites from polymers and layered minerals, *Acta Polymerica* **50**, 122-126.

Galgali, G., C. Ramesh and A. Lele, 2001, A rheological study on the kinetics of hybrid formation in polypropylene nanocomposites, *Macromolecules* **34**, 852-858.

Garcia-Leiner, M. A., 2004, Solid and melt state processing of polymers and their composites in supercritical carbon dioxide, Ph.D. Dissertation, University of Massachusetts, Amherst, MA.

Giannelis, E. P., 1996, Polymer layered silicate nanocomposites, *Adv. Mater.* **8**, 29-35.

Gilnian, J. W., T. C. L. Kashivagi, E. P. Giannelis, E. Manias, S. Lomakin, J. D. Lichtenhan, *et al.* In: M. Le Bras, G. Caniino, S. Bourbigot, R. Delobel, editors. 1998, Fire retardancy of polymers. Cambridge: The Royal Society of Chemistry.

Ke, Y. C., C. Long, and Z. Qi, 1999, Crystallization, properties, and crystal and nanoscale morphology of PET-clay nanocomposites, *J. Appl. Polym. Sci.* **71**, 1139-1146.

Kojima, Y. A., Usuki, M. Kawasumi, Y. Fukushima, A. Okada, T. Kurauchi and O. Kamigaito, 1993, Synthesis of nylon 6-clay hybrid, *J. Mater. Res.* **8**, 1179-1184.

Jimenez, G., N. Ogata, H. Kawai and T. Ogihara, 1997, Structure and thermal/mechanical properties of poly (ε-caprolactone)-clay blend, *J. Appl. Polym. Sci.* **64**, 2211-2220.

Lan, T., P. D. Kaviratna and T. J. Pinnavaia, 1995, Mechanism of clay tactoid exfoliation in epoxy-clay nanocomposites, *Chem. Mater.* **7**, 2144-2150.

Manke, C. W., E. Gulari, D. F. Mielewski and E. C. C. Lee, 2002, System and method of delaminating a layered silicate material by supercritical fluid treatment, U.S. Pat. 6,469,073 B1.

Mark, J. E., 1996, Ceramic-reinforced polymers and polymer-modified ceramics, *Polym. Eng. Sci.* **36**, 2905-2920.

Messersmith, P. B. and E. P. Giannelis, 1994, Synthesis and characterization of layered silicate-epoxy nanocomposites, *Chem. Mater.* **6**, 1719-1725.

Messersmith, P. B. and E. P. Giannelis, 1995, Synthesis and barrier properties of poly(ε-caprolactone)-layered silicate nanocomposites, *J. Polym. Sci., Part A: Polym. Chem.* **33**, 1047-1057.

Mielewski, D. F., E. C. C. Lee, C. W. Manke and E. Gulari, 2002, System and method of preparing a reinforced polymer by supercritical fluid treatment, U.S. Pat. 6,753,360 B2.

Novak, B. M., 1993, Hybrid nanocomposite materials - between inorganic glasses and organic polymers, *Adv. Mater.* **5**, 422-433.

Ogawa, M. and K. Kuroda, 1997, Preparation of inorganic-organic nanocomposites through intercalation of organoammonium ions into layered silicates, *Bull. Chem. Soc. Jpn.* **70**, 2593-2618.

Okada, A. and A. Usuki, 1995, The chemistry of polymer-clay hybrids, *Mater. Sci. Eng.* **C3**, 109-115.

Schmidt, H., 1985, New type of non-crystalline solids between inorganic and organic materials, *J. Non-Cryst. Solids* **73**, 681-691.

Solomon, M. J., A. S. Almusallam, K. F. Seefeldt, A. Somwangthanaroj and P. Varadan, 2001, Rheology of polypropylene/clay hybrid materials, *Macromolecules* **34**, 1864-1872.

Treece, M. A. and J. P. Oberhauser, 2007, Processing of polypropylene-clay nanocomposites: Single-screw extrusion with in-line supercritical carbon dioxide feed versus twin-screw extrusion, *J. Appl. Polym. Sci.* **103**, 884-892

Usuki, A., M. Kato, A. Okata and T. Kurauchi, 1997, Synthesis of polypropylene-clay hybrid, *J. Appl. Polym. Sci.* **63**, 137-139.

Vaia, R. A., H. Ishii and E. P. Giannelis, 1993, Synthesis and properties of two-dimensional nanostructures by direct intercalation of polymer melts in layered silicates, *Chem. Mater.* **5**, 1694-1696.

Xu, L., S. Reeder, M. Thopasridharan, J. Ren, D. A. Shipp and R. Krishnamoorti, 2005, Structure and melt rheology of polystyrene-based layered silicate nanocomposites, *Nanotechnology* **16(7)**, 514-521.

Zax, D. B., D.-K. Yang, R. A. Santos, H. Hegemann, E. P. Giannelis and E. Manias, 2000, Dynamical heterogeneity in nanoconfined poly(styrene) chains, *J. Chem. Phys.* **112(6)**, 2945-2951.